6-8-1997

Calculation of Electronic Coupling Matrix Elements for Ground and Excited State Electron Transfer Reactions: Comparison of the Generalized Mulliken–Hush and Block Diagonalization Methods

Robert J. Cave
Harvey Mudd College

Marshall D. Newton
Brookhaven National Laboratory

Calculation of electronic coupling matrix elements for ground and excited state electron transfer reactions: Comparison of the generalized Mulliken–Hush and block diagonalization methods

Robert J. Cave
Department of Chemistry, Harvey Mudd College, Claremont, California 91711

Marshall D. Newton
Department of Chemistry, Brookhaven National Laboratory, Upton, New York 11973

(Received 28 October 1996; accepted 25 February 1997)

Two independent methods are presented for the nonperturbative calculation of the electronic coupling matrix element (H_{ab}) for electron transfer reactions using *ab initio* electronic structure theory. The first is based on the generalized Mulliken–Hush (GMH) model, a multistate generalization of the Mulliken Hush formalism for the electronic coupling. The second is based on the block diagonalization (BD) approach of Cederbaum, Domcke, and co-workers. Detailed quantitative comparisons of the two methods are carried out based on results for (a) several states of the system $Zn_2OH_2^+$ and (b) the low-lying states of the benzene–Cl atom complex and its contact ion pair. Generally good agreement between the two methods is obtained over a range of geometries. Either method can be applied at an arbitrary nuclear geometry and, as a result, may be used to test the validity of the Condon approximation. Examples of nonmonotonic behavior of the electronic coupling as a function of nuclear coordinates are observed for $Zn_2OH_2^+$. Both methods also yield a natural definition of the effective distance (r_{DA}) between donor (D) and acceptor (A) sites, in contrast to earlier approaches which required independent estimates of r_{DA}, generally based on molecular structure data. © *1997 American Institute of Physics.*
[S0021-9606(97)00621-1]

I. INTRODUCTION

The electronic coupling between localized donor (D) and acceptor (A) sites can be an important factor in controlling the rates of electron transfer (et) reactions.[1] This is especially true in biological systems, where electrons transfer over large distances (>5 Å), generally assisted by the intervening medium.[2] In addition, the electronic coupling between different pairs of states of a given donor–acceptor pair often plays a role in determining the relative rates of transfers among the various states.[3] It is thus of critical importance to be able to estimate the electronic coupling matrix elements in order to understand the behavior of long distance electron transfer reactions. We denote such a coupling element as H_{ab}, where a and b refer generically to the initial and final diabatic states (i.e., the charge-localized valence bond structures which characterize the reactant and product states in the process of interest).[1] In contrast, adiabatic states (i.e., eigenfunctions of the electronic Hamiltonian) are denoted below by numerical labels (1,2,...).

A number of methods based on quantum chemical calculations have been proposed and applied to obtain estimates of H_{ab}. The determination of H_{ab} is a two-stage process involving first the specification of the states and, then the actual calculation of the coupling element. In many cases the coupling element between many-electron states (H_{ab}) may be replaced to a good approximation by the corresponding one-electron matrix element (H_{DA}) between local D and A orbitals.[1] Using electronic wave functions obtained either from semiempirical or *ab initio* techniques, previous studies[4–15] have evaluated and analyzed H_{ab} on the basis of various perturbative and nonperturbative approaches, often cast in terms of partitioning theory[5] or Green functions,[15] and involving either direct (i.e., in terms of localized states or orbitals) or indirect (i.e., splittings of delocalized state energies) treatments.[1] All of these studies have assumed the validity of the two-state approximation, in which the space of the two states of interest (i.e., either the diabatic states, ψ_a and ψ_b, or their adiabatic counterparts) is well separated energetically from the other states of the system.[1]

Approaches based on semiempirical quantum chemical methods are attractive because of the ease of application to large molecular systems, and the values obtained for H_{ab} are in reasonable agreement with results from *ab initio* calculations[8(c)] or from experiment[9,16] in cases where comparison has been made. Difficulties may however arise in application of such methods when nondynamical electron correlation effects[17] are important, especially in reactions involving excited states, or when parameters in the model are unavailable or insufficiently tested. In such cases it is important to be able to apply *ab initio* methods. Extensive application of *ab initio* methods has been made to study electron transfer in hydrocarbon systems[10–13] and systems involving metal atoms or ions.[7,8] Most studies have used Hartree–Fock (HF) wave functions and thus have been limited to reactions involving the lowest state of a given symmetry, but some studies have used correlated wave functions.[11(b),13] The H_{ab} values are obtained as: (i) one-half of the adiabatic state splitting in the case of symmetry-equivalent D and A groups;[10–13] (ii) the matrix element between the two nonor-

thogonal symmetry-broken diabatic states characterizing the initial and final states of the system,[7,8,12(b)] or (iii) the minimum splitting between two adiabatic states adjusted suitably by the application of an external field or variation of geometry.[11(b)] The first of these methods should be quite general whenever one is dealing with a symmetrical system, provided that the two-state model is adequate. The second method is generally applicable only in weakly coupled systems, and the inclusion of correlation can lead to ambiguities, since symmetry-breaking does not occur in the limit of fully correlated wave functions. Also, in the nonsymmetrical cases, in which the two diabatic states are not degenerate, averaging is required to maintain the Hermitian property of the coupling (i.e., $H_{ab}=H_{ba}$, where the matrix elements are real).[1] The third method is an attempt to circumvent the problems of the first two methods, but it is not always obvious which coordinates are best varied and/or whether one has reached the true minimum in splitting, especially for weakly coupled systems. When these problems are combined with the inherent difficulties in treating excited states, none of the above methods offers a fully satisfactory choice.

With the above limitations and difficulties in mind we have developed two alternative methods for calculating H_{ab}, which are broadly applicable to charge-transfer processes. Our criteria for acceptable methods of calculating H_{ab} are that they should:

(a) treat excited states as well as ground states,
(b) be capable of treating several states of interest simultaneously,
(c) be applicable to arbitrary molecular geometries, thereby allowing tests of the validity of the Condon approximation[1,2] (which neglects the variation of H_{ab} with respect to all molecular coordinates except those which affect the effective donor–acceptor separation distance, r_{DA}) and avoiding the need to search for the crossing of a pair of diabatic surfaces in order to calculate H_{ab}, and
(d) allow the inclusion of electron correlation for all states of interest.

Both methods presented here meet these four goals and they are, to our knowledge, the first methods to do so. The first approach is the generalized Mulliken–Hush approach, (GMH),[18] which uses a transformation of the adiabatic dipole moment matrix to define diabatic states. The second method (denoted below as BD) is based on block diagonalization[19] of the adiabatic Hamiltonian using configuration interaction (CI) coefficients obtained in a basis of configurations constructed in terms of a diabatic molecular orbital basis.[20] The applications reported here involve *et* processes occurring in the $Zn_2(H_2O)^+$ system[18(a)] and the benzene–chlorine atom contact ion-pair system.[21] The calculated results for these systems, which are dominated by direct [or ''through-space'' (TS)[1,7]] D/A coupling, allow critical comparisons of the GMH and BD methods.[22] We find that the two methods yield quite similar results and that either is a robust, general means for calculating H_{ab} for ground or excited state *et* processes. In addition to H_{ab}, the methods yield values of the effective distances separating D and A sites,[1(b),16,18(a)] defined as $r_{DA}=|\Delta\mu_{ab}|/e$, where $\Delta\mu_{ab}$ is the dipole moment difference for a pair of diabatic states, and e is the magnitude of the electron charge. These values of r_{DA} may be contrasted with previous estimates (r_{DA}^0) based on molecular structural or other empirical data.[18(c)–18(h)]

It should be emphasized that while we concern ourselves here with *ab initio* applications, either approach (GMH or BD) can also be applied using semiempirical methods, although in practice the GMH model is the easier of the two to apply in general. Lastly, as noted previously,[18(a)] since the GMH model is defined entirely in terms of adiabatic state properties (state energies, dipole moments, and transition moments), it can also be applied using purely experimental data to yield experimental estimates of H_{ab} and r_{DA}.

II. THEORETICAL METHODS

A. Generalized Mulliken–Hush method

The Mulliken–Hush method[18(c)–18(h)] for relating the adiabatic transition dipole moment, μ_{12}, to H_{ab} was originally derived for a two-state system with weakly interacting diabatic states, thus justifying the use of first order perturbation theory. In addition, it was assumed that the diabatic states were localized and that one could take $\mu_{ab}=0$. With this second assumption one could write the electronic coupling matrix element as

$$H_{ab}=\frac{|\boldsymbol{\mu}_{12}|\boldsymbol{\Delta}E_{ab}}{|\boldsymbol{\Delta}\boldsymbol{\mu}_{ab}|}, \tag{1}$$

where ΔE_{ab} is the diabatic state energy gap, approximated by the observed (adiabatic) excitation energy (ΔE_{12}) for optical *et*, with μ_{12} and $\Delta\mu_{ab}$ (i.e., the diabatic dipole moment difference) taken as scalar quantities since it is assumed that all dipole vectors are collinear, aligned along a direction defined by the centroids of the D and A orbitals. Since the diabatic states are not known in general, the Mulliken–Hush treatment makes a third assumption, namely that $|\Delta\mu_{ab}|$ in the denominator of Eq. (1) can be approximated by er_{DA}^0, where r_{DA}^0 is generally inferred from structural data, as noted in Sec. I. It has recently been shown[18(g),18(h)] that Eq. (1) may be extended to the nonperturbative regime by replacing ΔE_{ab} with ΔE_{12}.

In the generalized Mulliken–Hush (GMH) model[18(a)] we retain the assumption that the diabatic states localized at different sites have zero off-diagonal dipole moment matrix elements, and exploit this assumption as a means of defining diabatic states in an n state framework. The method is not restricted to a perturbative treatment (within the n states of interest), nor is there a need to approximate $\Delta\mu_{ab}$ in terms of structural data (i.e., r_{DA}^0, as noted above) in order to obtain H_{ab}. In fact, the GMH model yields directly a value for $\Delta\mu_{ab}$ as well as H_{ab}.

The GMH model takes as its starting point the vector components of the dipole moment matrix and the energy eigenvalues (i.e., the diagonal Hamiltonian matrix) for the desired manifold of n adiabatic states. The GMH analysis

employs only the vector component of each dipole matrix element in the direction defined by the dipole difference vector for the initial and final adiabatic states (two-state case) or by the average of such differences when several *et* processes are considered for a given system.[16,18(a)] As a first step we diagonalize this dipole moment matrix ($\boldsymbol{\mu}^{\mathbf{ad}}$) and apply the same transformation to the adiabatic (i.e., diagonal) Hamiltonian matrix. However, full diagonalization of $\boldsymbol{\mu}^{\mathbf{ad}}$ is too restrictive since the central assumption of the GMH model requires $\mu_{ab}=0$ *only* for state pairs a,b in which the transferring electron is localized on different sites. Since the processes under investigation here are of the long-range *et* type, one can easily group the eigenfunctions of the dipole matrix into blocks associated with different localization sites, as defined by the corresponding eigenvalues. Within each block we then diagonalize the Hamiltonian, thus obtaining states which are *adiabatic* within a given local block, but still *diabatic* with respect to states localized at different sites.[18(a)] Applying the same block-by-block transformation to the diagonal dipole moment matrix yields the diabatic state dipole moments (μ_{aa}) and transition moments within each local block.

The formulation of the GMH given above was cast in terms of a general n-state system involving long-range *et*. In the limiting case of a two-state *et* system one obtains the following GMH results:

$$|H_{ab}|=|\boldsymbol{\mu}_{12}|\boldsymbol{\Delta E}_{12}/|\boldsymbol{\Delta\mu}_{ab}|, \tag{2a}$$

$$|\boldsymbol{\Delta\mu}_{ab}|=[(\boldsymbol{\mu}_{11}-\boldsymbol{\mu}_{22})^2+4(\boldsymbol{\mu}_{12})^2]^{1/2}, \tag{2b}$$

displaying explicitly the manner in which the diabatic quantities (H_{ab} and $\Delta\mu_{ab}$) may be expressed *entirely* in terms of adiabatic state information. This reliance exclusively on adiabatic states applies, of course, to the general n-state situation as well as the simple two-state case and allows one to evaluate H_{ab} and r_{DA} (i.e., $|\Delta\mu_{ab}|/e$) using either the output of conventional quantum chemistry codes or experimental data.[1(b),16,18(a)] Finally, it should be clear that the GMH procedure can be performed at any geometry, not merely that corresponding to degeneracy of the diabatic states (in which case they are mixed 50/50 in the corresponding adiabatic states).

Previous examples of the use of diagonalization of the dipole moment matrix in defining diabatic states have been discussed in recent literature, but applied in a pairwise fashion.[23]

B. Block diagonalization of the adiabatic electronic Hamiltonian

The block diagonalization (BD) procedure outlined here closely follows the methods developed by Cederbaum *et al.*[19] and Domcke *et al.*[20] but with particular focus on diabatic states suitable for representing in a chemically intuitive manner (i.e., in terms of ''valence bond'' structures), the initial and final states (and possibly intermediate states) pertinent to *et* processes, as introduced in Sec. I. Diabatic states defined in this manner, in contrast to the adiabatic states (i.e., those which diagonalize the electronic Hamiltonian), are expected to vary slowly with respect to nuclear coordinates, and thus their matrix elements over the nuclear momentum and kinetic energy operators are generally quite small.[19,20,24] The BD approach can be applied to any configuration interaction (CI) wave function and associated electronic Hamiltonian matrix, while the extension of the method by Domcke *et al.*[20] relies on the use of a state-averaged complete active space self-consistent field wave function (denoted below as nSA/CASSCF where n indicates the number of states averaged in the orbital optimization).[25] This latter method allows a multistate treatment with a common set of orbitals, a property of great convenience in the formulation of a diabatic electronic Hamiltonian with eigenvalues identical to the original adiabatic state energies[20] (in the following, ''Hamiltonian'' is understood to refer to the electronic Hamiltonian, denoted H).

1. Definition of diabatic states

In implementing the BD approach for *et* processes of interest in any given system, we first obtain the desired set of diabatic states, $\{\psi_j^{P_0}\}$, for a corresponding zeroth-order reference system. This set, $\{\psi_j^{P_0}\}$, denoted collectively as the P_0-space, of dimension $n_P\geqslant 2$, a subspace of the nSA/CASSCF space ($n_P\leqslant n$), includes the important valence-bond structures of the type described above (i.e., the appropriate charge-localized states). For each bimolecular *et* system discussed below, the zeroth-order reference system (denoted by the coordinate set $\{\mathbf{x}^0\}$) is chosen as the ''noninteracting'' system in which the two reactants are at large separation (for intramolecular *et*, alternative noninteracting systems may be defined[26]). In the noninteracting reference systems, each of the relevant n_P adiabatic solutions, $\Psi_j^{P_0}$, selected from the nSA/CASSCF space ($n_P\leqslant n$), when expressed in terms of a suitable set of diabatic orbitals, as described below, is found typically to be strongly dominated by a single (or, in some cases, a few) charge-localized electronic configuration X_j^0 (taken here as a spin-adapted set of single-determinants associated with a given electronic configuration) denoted below as a configuration state function (CSF).[27] Taking this set of n_P CSF's as the reference diabatic states ($\psi_j^{P_0}=X_j^0$, $j=1$ to n_P), we obtain the desired diabatic set $\{\psi_j^P\}$ at the geometry of interest (denoted collectively as $\{\mathbf{x}\}$) in a ''least-motion'' fashion[19] by projecting the $\{\psi_j^{P_0}\}$ onto the corresponding space (P) of n_P adiabatic states, $\{\Psi_j^P\}$, from the nSA/CASSCF calculation for the system at $\{\mathbf{x}\}$. The direct result of this projection (for which details are given below) may be represented as

$$(\psi_j^P)'=\sum_k^{n_P}\Psi_k^P C'_{kj}, \quad j=1,n_P, \tag{3a}$$

where

$$C'_{kj}\equiv\langle\Psi_k^P|\psi_j^{P_0}\rangle. \tag{3b}$$

(In view of the foregoing the $\psi_j^{P_0}$ may be referred to as ''projectors''.) Since the finite P space does not provide a complete basis, the C'_{kj} do not yield an orthonormal set

$\{(\psi_j^P)'\}$. For convenience, we orthonormalize the $\{(\psi_j^P)'\}$, maintaining the ''least motion'' approach by applying a Löwdin transformation[28]

$$\psi_j^P = \sum_k^{n_P} (\psi_k^P)' S_{kj}^{-1/2} = \sum_k^{n_P} \Psi_k^P U_{kj}, \quad j=1,n_P, \tag{4a}$$

where

$$S_{kj} \equiv \langle (\psi_k^P)' | (\psi_j^P)' \rangle = \sum_m^{n_P} C'_{mk} C'_{mj}, \tag{4b}$$

and where **U** is a unitary matrix, an alternative to the unitary transformation defined by the GMH procedure discussed above.

2. Diabatic hamiltonian

Dividing the total many-electron space associated with the nSA/CASSCF calculation for the system of interest (i.e., at $\{\mathbf{x}\}$) into the P-space and the remainder (denoted as the Q space),[29] we see that the least-motion transformation yielding $\{\psi_i^P\}$ casts the Hamiltonian in block diagonal form (with respect to the P and Q space blocks). The variational nature of the nSA/CASSCF procedure guarantees that all Hamiltonian coupling elements between the P space and the Q space are zero. The generally nondiagonal diabatic Hamiltonian matrix ($\mathbf{H^P}$) in the P space is given by

$$H_{jk}^P = \langle \psi_j^P | H | \psi_k^P \rangle = (\mathbf{U^\dagger \Lambda^P U})_{jk}, \quad j,k=1,n_P, \tag{5}$$

where Λ^P is the (diagonal) adiabatic Hamiltonian in the P space, with elements $\Lambda_{jk}^P = \langle \Psi_j^P | H | \Psi_j^P \rangle \delta_{jk}$, $j=1,n_P$, where $\{\Psi_j^P\}$ is the set of adiabatic states introduced above [see Eq. (3a)], and where **U** is defined by Eq. (4a). Since **U** is unitary, H_{ij}^P is easily seen to preserve the P-space nSA/CASSCF energies.

3. Relationship between diabatic states and the noninteracting reference states

While the projection scheme just outlined yields diabatic states (ψ_j^P) as ''close as possible'' (as obtained by ''least motion''[19]) to the reference set, $\psi_j^{P_0}$, we emphasize the crucial physical distinction between the two sets. The reference set is strongly charge-localized: e.g., the pair of states in the reference set which corresponds to the initial and final states in the et process of interest, which we denote as ψ_D^0 and ψ_A^0, will have the transferring electron strongly localized, respectively, in a donor (ϕ_D^0) and an acceptor (ϕ_A^0) orbital. The direct (TS) coupling[1,7] between ϕ_D^0 and ϕ_A^0, and hence also ψ_D^0 and ψ_A^0, will generally be negligible at the reference geometry ($\{\mathbf{x}^0\}$), but may attain appreciable magnitude after translation so as to correspond to the geometry of the system of interest ($\{\mathbf{x}\}$). Further substantial modification of the coupling strength may occur as a result of the subsequent projection [Eq. (4a)] of the reference diabatic states onto the adiabatic P-space (for $\{\mathbf{x}\}$), which implicitly ''dresses'' the zeroth-order reference states with contributions from outside the reference (P_0) space, thus yielding the effective D/A coupling element

$$H_{DA}^P \equiv \langle \psi_D^P | H | \psi_A^P \rangle. \tag{6}$$

The most important role of the ''dressing'' is to include hybridization or polarization effects, and when D and A are separated by solvent or spacer groups, to incorporate superexchange pathways[1] involving excess electrons or holes at sites in the spacer between the D and A sites. When an intervening medium is present, superexchange coupling generally provides the dominant mechanism for D/A coupling in long-range et. Dressing of the $\{\psi_j^{P_0}\}$ may also involve electron correlation contributions, although such effects typically do not have a major influence on H_{DA} magnitudes,[1(b)] and are expected to be small contributors (relative to the dressing of the direct DA coupling due to superexchange) when superexchange effects are present.

4. Choice of active space orbitals

The reference (noninteracting) diabatic states, $\psi_j^{P_0}$, defined above in terms of specific CSFs in the nSA/CASSCF wave functions are, of course, contingent on the choice of active space orbitals. We recall that while CASSCF wave functions and energies are invariant with respect to an arbitrary rotation of orbitals within the active space (since a full CI is carried out within the active space), the constituent CSFs, the dominant members of which define the $\psi_j^{P_0}$ set, obviously depend on the choice of orbitals used to represent the nSA/CASSCF wave function. We have obtained a suitable set of charge-localized $\psi_j^{P_0}$ diabatic wave functions by choosing as orbitals the average natural orbitals (ANO's) associated with the nSA/CASSCF states.[30,31] In general, the ANO's for the noninteracting $\{\mathbf{x}^0\}$ reference system are strongly localized on the different sites associated with the et process. In the special case of symmetry equivalent D/A sites, the ANO's will be delocalized. However, in this case they occur in essentially degenerate symmetric–antisymmetric pairs (where we refer to the degeneracy of the eigenvalues of the nSA/CASSCF density matrix), and localized ANO pairs are straightforwardly obtained by taking the plus and minus combinations of the members of each quasidegenerate pair.

5. Computational implementation

In projecting the reference diabatic states, $\psi_j^{P_0}$, onto the adiabatic space of interest (i.e., the set $\{\Psi_j^P\}$), as displayed in Eq. (3), we employ the procedure reported in Ref. 20; i.e., in order to simplify the computational implementation of Eq. (3), the reference CSFs (X_j^0), defined in terms of the reference diabatic orbitals, $\{\phi_j^0\}$ (the ANO's, as described above), are replaced to good approximation by the corresponding CSFs defined in terms of orbitals obtained by projecting the $\{\phi_j^0\}$ onto the orbital space of the system of interest (i.e., at $\{\mathbf{x}\}$) as follows: the active space reference ANO's are projected[20] onto the active space of orbitals from the nSA/CASSCF calculation for the $\{\mathbf{x}\}$ system and then orthonormalized in a ''least motion'' fashion by the Löwdin transformation[28] [analogous to that given in Eq. (4)]. Formally, one could treat the inactive [doubly occupied orbitals

TABLE I. Ionization energies for separate species (eV).[a]

State[b]	Zn	$ZnOH_2$ (3.05 Å)[c]	$ZnOH_2$ (2.05 Å)[c]
1^1S	8.55 (9.39)[d]	7.77	6.68
1^3P	5.04 (5.34)[d]	3.86	3.29

[a]Neutral species obtained based on 2/5 CASSCF calculations (see the text), with ions based on SCF.
[b]For molecular species the state designation is the atomic state of Zn to which the molecular state would correlate at large r_{ZnO}. This is in all cases the lowest state of the given spin symmetry at the given distance.
[c]The Zn–O distance is given in parentheses.
[d]Experimental values (Ref. 40) are given in parentheses.

(the core)] in a similar fashion, but since the CASSCF CI coefficients are invariant to a rotation of the core space one may simply employ any convenient orbital representation of the core orbital space for the system at $\{\mathbf{x}\}$. With these approximations, the projection in Eq. (3) is easily carried out (since all matrix elements involve a common orthonormal basis), thus yielding [via Eqs. (4) and (5)] the desired diabatic Hamiltonian ($\mathbf{H}^P$) at $\{\mathbf{x}\}$.

C. Choice of state space

The two approaches delineated above have the important advantage of generality with respect to the size of state space adopted [denoted, respectively, as n (GMH) and n_P (BD)]. The choice of optimal size depends, of course, on the details of the system investigated, as exemplified in Sec. IV, but is guided in general by considerations of compactness (i.e., as small as possible, subject to the constraint of adequately spanning the space of states important for the processes of interest) and energy separation (i.e., being adequately separated energetically from the states outside of the primary space).

TABLE II. Electronic coupling elements vs distance for Zn_2^+.[a]

r_{ZnZn} (Å)	Method	$H_{ss'}$	$H_{pp'}$	$H_{sp'/ps'}$
5.0	GMH	7.26	13.9	24.4
	BD	6.15	12.8	18.7
6.0	GMH	2.16	7.07	10.8
	BD	2.04	6.94	8.03
7.0	GMH	0.623	3.41	4.49
	BD	0.610	3.39	3.36
8.0	GMH	0.171	1.54	1.80
	BD	0.170	1.54	1.38
9.0	GMH	0.0440	0.651	0.704
	BD	0.0338	0.651	0.553
β	GMH	2.55	1.53	1.78
	BD	2.58	1.49	1.76

[a]GMH and BD matrix elements reported in mhartrees, and labeled by the dominant Zn valence orbitals involved in the coupling, based on 3/8 4SA/CASSCF calculations as discussed in the text (one of the two equivalent Zn atoms is distinguished by a ''prime''). All H_{ab} quantities listed in Tables II, III, and V–VII correspond to the *magnitudes* of the coupling elements.
[b]β values come from fits of the data to the forms $H_{ab}=A\exp(-\beta r/2)$, where $r=r_{ZnZn}$.

III. COMPUTATIONAL DETAILS

A. Many-electron wave functions

Except for the results of Table I, all the wave functions used were state-averaged CASSCF wave functions (i.e., nSA/CASSCF;[25] however, neither method (GMH or BD) is limited to this choice of wave function. In Table I single-state CASSCF results are reported. The CASSCF calculations are denoted as l/m CASSCFs, where l denotes the number of electrons correlated and m denotes the size of the active orbital space used in the calculation. All calculations were performed using the MOLCAS software.[32]

B. Structural model and one-electron basis sets

1. Zn_2^+ and $Zn_2OH_2^+$

The basis set used to describe the Zn atom is obtained from the Wachters $(14s,9p,5d)$ set.[33] The $14\,s$ functions, $9\,p$ functions, and $5\,d$ functions were contracted using a Raffenetti scheme[34] based on the coefficients supplied in Ref. 33, yielding $4\,s$, $2\,p$, and $1\,d$ contracted functions, respectively. The two most diffuse s functions and the most diffuse p and d functions of the original set were also added as independent uncontracted functions. Finally, we included two additional s functions (0.3960,0.015), $4\,p$ functions (0.310, 0.120, 0.047, 0.018) and $1\,d$ function (0.155).[35] Tests were performed augmenting the above Zn basis with more diffuse s, p, and d functions. At the largest Zn–Zn separations examined here ($r_{Zn-Zn}=9$ Å), the largest change in a coupling matrix element due to the increased basis set size was 12%. Thus it was felt the above basis set was adequate for the present study.

For essentially all of the geometries examined here the CASSCF wave functions for Zn_2^+ are stable with respect to symmetry breaking. In order to perturb the symmetry equivalence of the two Zn atoms in a controlled fashion a water molecule was added on the periphery of the Zn_2^+ molecule so as to form a C_{2v} $Zn_2(H_2O)^+$ complex (with the H_2O twofold axis collinear with the Zn_2^+ axis, and with the negative (O) end of the water closest to the Zn_2^+ moiety). The water molecule was assigned the experimental[36] equilibrium structure ($r_{OH}=0.957$ Å and $\sphericalangle HOH=104.5°$). Variation of the distance between O and the nearest Zn atom (r_{ZnO}), was used to control the degree of symmetry-breaking (within the local Zn_2^+ unit) and to allow a test of the Condon approximation.[1,2] To sample states near the $Zn(OH_2)$ minimum we used $r_{ZnO}=3.05$ Å, which is near the calculated equilibrium distance for the neutral species. For this limited purpose it was felt adequate to employ a minimal atomic natural orbital basis set for water.[37] The main role of the water molecule in these model calculations is to shift the Zn energy levels, although some donation of charge to the water was observed in excited states of $Zn_2(H_2O)^+$, even with the minimal basis. Of course, the $Zn_2(H_2O)^+$ system may be considered an *et* system of potential interest in its own right, warranting further study employing more flexible water basis sets.[38] Most of the

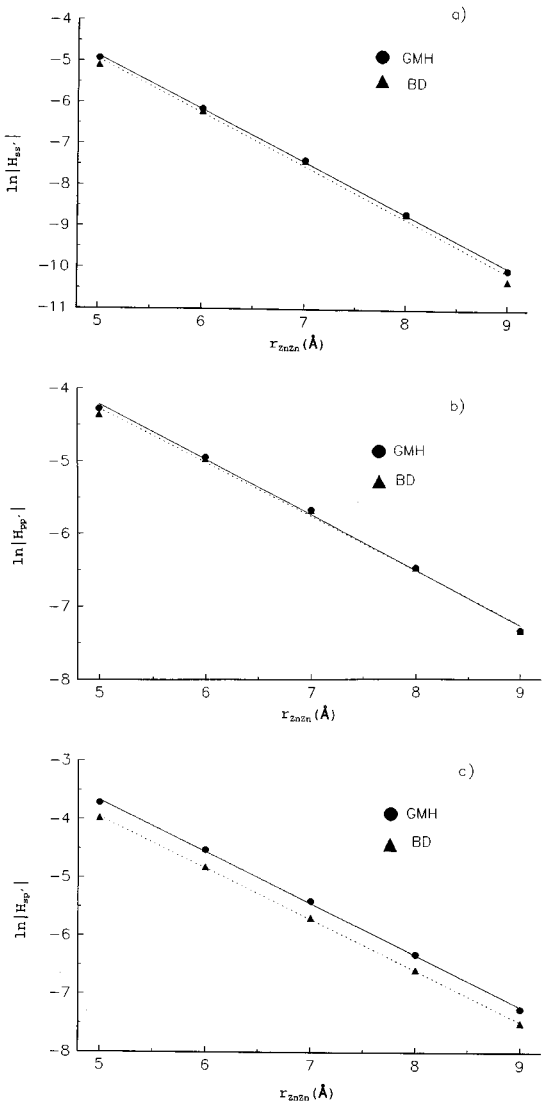

FIG. 1. Plot of $\ln|H_{ab}|$ vs r_{ZnZn} for Zn_2^+ based on the GMH (circles) and BD (triangles) methods: (a) $H_{ss'}$, (b) $H_{pp'}$, (c) $H_{sp'}$.

calculations reported below were carried out for $r_{\mathrm{ZnO}}=2.05$ or 3.05 Å, near the calculated equilibrium values, respectively for ZnH_2O^+ and ZnH_2O.

2. Benzene+Cl atom

A split valence (VDZ) atomic natural orbital[37] basis was used on all atoms. The five states of interest (the lowest five) were described with a 9/5 5SA/CASSCF (comprising the three close-lying states of benzene plus chlorine, and two low-lying excited states corresponding to *et* from either of the two π HOMOs of benzene to the chlorine p shell). The geometries used for the present comparative study of the GMH and BD methods had benzene centered at the origin in the xy plane, with the x axis bisecting two parallel CC bonds. The Cl atom was placed in a plane a distance $r=3$ Å above the xy plane at two different distances (d) along the x axis [$d=1.208$ Å, centered above a CC bond (in a ''π complex''[18(a),21])], and $d=0.6$ Å).[39] We obtain three distinct matrix elements, corresponding to transfer from benzene to (a) the Cl p_z orbital (pointing at the ring), (b) the Cl p_y orbital, and (c) the Cl p_x orbital. Symmetry dictates the member of the nearly degenerate pair of highest occupied orbitals on benzene from which the electron is removed in each case (i.e., a' or a'' in the C_s point group).

IV. RESULTS

A. $Zn^{0/+}$ and $Zn(H_2O)^{0/+}$

Prior to dealing with the full clusters, Zn_2^+ and $Zn_2(H_2O)^+$, we consider the ionization energies of the constituent units, Zn and $Zn(H_2O)$. In Table I we report the ionization energies (IP) of Zn and ZnH_2O from their two lowest electronic states. For the neutral Zn species we performed 2/5 CASSCF calculations, which for the ground-state amounts to correlation of the $4s$ electron pair on Zn via excitation into the $4p$ and $5s$ orbitals. In ZnH_2O the active space has similar character, but for Zn–O distances in the 2 to 3 Å range there is significant water character to the correlating orbitals, as well as some $4s-4p_z$ mixing (Zn–O lies along the z axis) in the nominally doubly occupied orbital. For the ions we performed single-configurational open shell SCF calculations (no correlation being required for the unpaired electron) as the appropriate counterparts to the neutral 2/5 CASSCF calculations. The IPs are of interest since they yield some estimate of the decay with distance of the highest occupied orbital in the neutral species, and thus should be related to the decay with distance of the electronic coupling matrix element[7] (see below). The calculated IPs for Zn are found to be within 1 eV of experimental values.[40]

B. Zn_2^+ and $Zn_2(H_2O)^+$

We now consider the coupling elements which encompass the various electron transfer processes between the valence s and p orbitals of the two Zn atoms in the Zn_2^+ and $Zn_2(H_2O)^+$ systems (we focus specifically on orbitals of ''sigma'' symmetry (i.e., a_1 in C_{2v} point-group symmetry). A minimal representation of these processes, which include thermal (from ground or photoexcited states) and optical transfer, requires inclusion of the four lowest-energy states of appropriate symmetry for each system [$^2\Sigma_g$ or $^2\Sigma_u$ for Zn_2^+, and $^2A_1$ for $Zn_2(H_2O)^+$]. While these processes from a fundamental point of view involve many-electron rearrangements, they may typically be cast to a good approximation as effective one-electron (or one-hole) transfers between D and A orbitals.[1,8(b)] In this spirit, we employ an obvious orbital notation in labeling the following processes connecting the various diabatic states (identified by the dominant Zn and Zn^+ valence states):

$$\mathrm{Zn}(^1S)+\mathrm{Zn}^+(^2S)\rightarrow\mathrm{Zn}^+(^2S)+\mathrm{Zn}(^1S)\quad s\rightarrow s', \tag{7a}$$

$$\mathrm{Zn}(^3P)+\mathrm{Zn}^+(^2S)\rightarrow\mathrm{Zn}^+(^2S)+\mathrm{Zn}(^3P)\quad p\rightarrow p', \tag{7b}$$

$$\mathrm{Zn}(^1S)+\mathrm{Zn}^+(^2S)\rightarrow\mathrm{Zn}^+(^2S)+\mathrm{Zn}(^3P)\quad s\rightarrow p', \tag{7c}$$

$$\mathrm{Zn}(^3P)+\mathrm{Zn}^+(^2S)\rightarrow\mathrm{Zn}^+(^2S)+\mathrm{Zn}(^1S)\quad p\rightarrow s', \tag{7d}$$

TABLE III. (a) Electronic coupling elements vs distance (r_{ZnZn}) for $Zn_2H_2O^+$ with $r_{ZnO}=2.05$ Å.[a] (b) Electronic coupling elements vs distance (r_{ZnZn}) for $Zn_2H_2O^+$ with $r_{ZnO}=3.05$ Å.[a]

r_{ZnZn} (Å)	Method	$H_{ss'}$	$H_{pp'}$	$H_{sp'}$	$H_{ps'}$
		(a)			
4.0	GMH	28.3	23.6	50.4	42.7
	BD	18.2	14.9	39.0	46.3
5.0	GMH	10.5	13.0	51.7	22.3
	BD	6.28	9.60	30.4	23.0
6.0	GMH	3.73	7.55	41.1	10.1
	BD	2.03	6.47	21.3	10.6
7.0	GMH	1.09	4.23	21.8	4.08
	BD	0.804	3.79	12.8	4.33
8.0	GMH	0.340	2.57	13.8	1.62
	BD	0.274	2.27	7.32	1.78
9.0	GMH	0.0958	1.44	7.36	0.611
	BD	0.0921	1.22	3.64	0.710
β[b]	GMH	2.28	1.11	0.81	1.71
	BD	2.10	0.99	0.95	1.68
		(b)			
4.0	GMH	29.7	34.4	59.3	41.7
	BD	14.0	18.6	56.8	44.8
5.0	GMH	7.95	14.7	38.5	22.1
	BD	5.62	12.4	30.6	21.8
6.0	GMH	2.34	7.83	19.1	9.44
	BD	2.01	7.37	16.0	9.48
7.0	GMH	0.698	4.25	9.56	3.84
	BD	0.655	4.17	8.80	4.00
8.0	GMH	0.203	2.27	4.78	1.51
	BD	0.196	2.25	4.56	1.70
9.0	GMH	0.0558	1.16	2.32	0.574
	BD	0.0529	1.14	2.19	0.707
β[b]	GMH	2.49	1.32	1.32	1.74
	BD	2.23	1.12	1.29	1.67

[a]The results (in mhartree) were obtained from 3/12 4SA/CASSCF calculations. See the text and footnote a of Table II for state designations. Table I of Ref. 18(a) listed similar β values (based on the 5–9 Å range of r_{ZnZn}). The ''prime'' on the orbital labels denotes the Zn atom closest to the water ligand.

[b]See footnote b of Table II for details.

where s and p denote valence $4s$ and $4p\sigma$ (i.e., $4p_z$) orbitals and where a ''prime'' is used to distinguish the two Zn sites [for the case of $Zn_2(H_2O)^+$, the ''prime'' denotes the Zn atom closest to the H_2O (see Sec. III)]. The sp' and ps' matrix elements are equal by symmetry[41] for Zn_2^+ [and, of course, for $Zn_2(H_2O)^+$ with $r_{ZnO}=\infty$].

The description of the above processes [Eq. (7)] as effectively one particle in nature requires not only that the *overall* spin state is conserved but also that no additional electronic excitations (''shakeup'') occur [e.g., as discussed in Ref. 8(d)]. These conditions are all satisfied in the present study. While all of the calculations reported here were for doublet states (as noted above), for process (7b) an overall quartet state would also be possible. In the case of states involving excited neutral Zn atoms, we note that of the two independent doublet states possible for the important CSF's with three singly occupied orbitals, the CSF with local $Zn(^3P)$ character is strongly dominant in the CASSCF wave functions.

The reference (noninteracting) states in the BD method (i.e., the ''projectors'') were obtained from the nSA/CASSCF calculations for $r_{ZnZn}=20$ Å, taken as the dominant CSFs for each state[27] (expressed in terms of ANO's, as discussed in Sec. II B).

1. Zn_2^+

In Table II we report electronic coupling matrix elements based on both the GMH and BD methods for the Zn_2^+ system. We used 3/8 4SA/CASSCF wave functions (4 orbitals per center, corresponding to the $4s$ and $4p$ set at large r_{ZnZn} and r_{ZnO}). [In Ref. 8(a) we used a 3/10 space for the Zn_2^+ calculations, which adds an extra s-like correlating orbital on each center. Little difference is found in the electronic coupling elements obtained with the two spaces.] For both GMH and BD methods the matrix elements show significant variation with orbital type, as do the various decay rates with distance (see β values in Table II). The linear fits of $\ln|H_{ab}|$ vs r_{ZnZn} (see Fig. 1) were quite good, with linear regression coefficients of $r\geqslant 0.995$ (the only exceptions being the $H_{sp'}$ matrix elements for $r_{ZnO}=2.05$ Å, where there are significant deviations from linearity, and r is ~ 0.95). It is of interest to note that the trends in β are the same as those in IP values for the local neutral donor group [$Zn(^1S)$ and $Zn(^3P)$], as expected from the semiclassical expression for tunneling through a homogeneous barrier.[1,7]

$$\beta=2[2m(\mathrm{IP})/\hbar^2]^{1/2}. \tag{8}$$

Using the IP's listed in Table I yields $\beta_{s,s'}=3.00$ Å^{-1} and $\beta_{p,p'}=2.30$ Å^{-1}, in the same order but significantly larger than those obtained from the detailed quantum calculations. While the simple model underlying Eq. (8) does not directly permit an estimate of β for the ''cross reactions'' [Eqs. (7c) and (7b)], the fact that $\beta_{sp'/ps'}$ is closer in magnitude to $\beta_{pp'}$ than to $\beta_{ss'}$ is qualitatively consistent with the notion that the decay is dominated by the ionization energy associated with the highest-lying (or most spatially diffuse) orbital involved in the et process.

The GMH and BD methods yield quite similar results for the $s-s'$ matrix elements at all distances examined. The same is true for the $p-p'$ matrix elements. The GMH $s-p'/p-s'$ matrix element is uniformly about 30% higher than that from the BD method, but the β values are quite similar.

For the $s-s'$ and $p-p'$ matrix elements for Zn_2^+, a third estimate comes from taking half the splitting between the relevant symmetric and antisymmetric adiabatic states.[1] The resulting values of $H_{ss'}$ (in mhartree) are: 6.35 (5.0 Å); 2.08 (6.0 Å); 0.617 (7 Å); 0.171 (8 Å); 0.0440 (9 Å), with r_{ZnZn} values in parentheses. The values of $H_{pp'}$ (in mhartree) are: 13.0 (5.0 Å); 6.99 (6.0 Å), 3.41 (7 Å); 1.54 (8 Å); $1.54e-3$; 0.651 (9 Å). These latter results are in quite good agreement with those obtained from either of the four-state methods, with values in each case lying between the GMH and BD values. The splitting approach is not directly applicable to the cross reactions, where no pairwise (i.e., 2-state) ap-

proach is possible in an adiabatic basis (in the absence of some artificial external perturbation) and the full (i.e., four-state) GMH or BD is required in general.

2. $Zn_2(H_2O)^+$

a. H_{ab} In Table III we present results for $Zn_2H_2O^+$ with $r_{Zn-O}=2.05$ Å (Table III A) or 3.05 Å (Table III B) for a range of r_{Zn-Zn} in each case. A 3/12 4SA/CASSCF describing the four lowest states of the system was used. The 12 active space orbitals correspond to the $4s$, $4p$ spaces on each Zn (the 3/8 space), with an extra s and p_z pair on each center to allow for shape changes in the neutral and cation s and p_z orbitals. Unlike the case of Zn_2^+ discussed above (corresponding in the present context to $r_{ZnO}=\infty$), none of the $Zn_2(H_2O)^+$ energy levels at large r_{ZnZn} approach near-degeneracy for finite values of r_{ZnO} (this contrast is illustrated by the energy gaps for Zn_2^+ and $Zn_2(H_2O)^+$ displayed in Table IV for a variety of geometries). The following adiabatic state ordering is observed: (1) $Zn(^1S)+Zn{-}OH_2^+(^2S)$; (2) $Zn^+(^2S)+Zn{-}OH_2(^1S)$, (3) $Zn(^3P)+Zn{-}OH_2^+(^2S)$, and (4) $Zn^+(^2S)+Zn{-}OH_2(^3P)$. In the state designations for $ZnOH_2^{+/0}$ we use the atomic state of Zn with which the complex would correlate were the water removed to large distance. These designations are the same as the diabatic state labels introduced above, in connection with Eq. (7) (although the degree of charge localization is greater for the diabatic states), except in the limit of very large r_{ZnO} (where adiabatic states approach symmetric delocalization with respect to the Zn_2^+ moiety). The inequivalence of the two Zn atoms (for finite r_{ZnO}) leads to distinct values for $H_{sp'}$ and $H_{ps'}$. In addition to the four *et* processes [Eq. (7)], we note that the one-center transitions, $s-p$ and $s'-p'$, which would be spin forbidden for large r_{Zn-Zn}, have small but finite transition moments in general due to the overall doublet spin state of the system (the so-called trip doublets[42]).

TABLE IV. Energy separations for the four lowest adiabatic states of $Zn_2OH_2^+$ and Zn_2^+ vs r_{Zn-Zn}.[a]

System	r_{Zn-Zn}	r_{Zn-O}	ΔE_{1-2}	ΔE_{2-3}	ΔE_{3-4}
$Zn_2OH_2^+$	9.0	2.05	1.74	1.69	1.76
	5.0	2.05	1.38	2.15	1.58
	9.0	3.05	0.69	2.74	1.06
	5.0	3.05	0.64	2.74	1.07
Zn_2^+	9.0	⋯	0.002	3.27[b]	0.04
	5.0	⋯	0.35	2.80	0.71

[a]All energy differences in eV; see text for valence-bond designations of states. The $Zn_2OH_2^+$ results are from 3/12 4SA/CASSCF calculations, while the Zn_2^+ results are from 3/8 4SA/CASSCFs. For comparison with the separated systems of Table I, the sum of $\Delta E_{1,2}$ and $\Delta E_{2,3}$ is the ground singlet–excited triplet splitting on the Zn atom in the presence of $ZnOH_2^+$, while the sum of $\Delta E_{2,3}$ and $\Delta E_{3,4}$ is the corresponding splitting of $ZnOH_2$ in the presence of the Zn^+ cation.

[b]This value differs slightly from the value of 3.40 eV given in the text of Ref. 18(a) [based on a slightly larger active space (3/10)].

b. Decay coefficients (β). The GMH and BD methods yield similar values for the matrix element of each orbital type (with the agreement being better at large r_{ZnZn}) and also similar decay with r_{ZnZn} (ie., β), as seen in Table III and Figs. 2 and 3. The β values for $Zn_2(H_2O)^+$ are uniformly

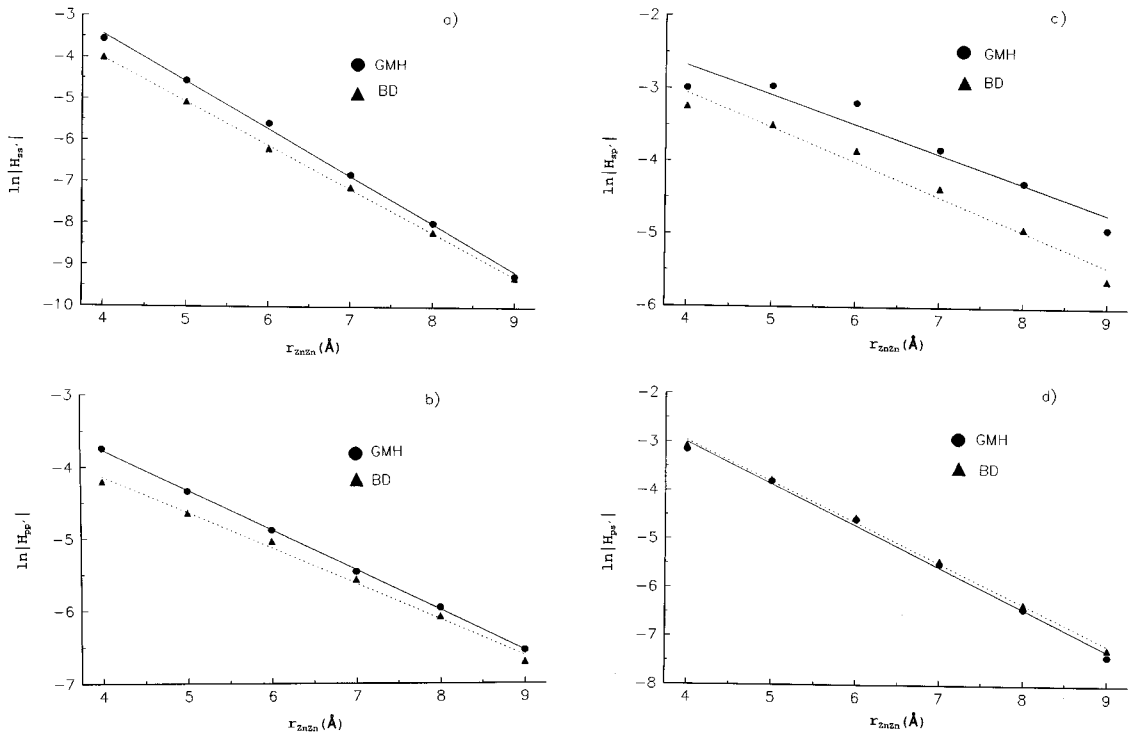

FIG. 2. Plot of $\ln|H_{ab}|$ vs r_{ZnZn} for $Zn_2(H_2O)^+$ based on the GMH (circles) and BD (triangles) methods, with $r_{ZnO}=2.05$ Å: (a) $H_{ss'}$, (b) $H_{pp'}$, (c) $H_{sp'}$, (d) $H_{ps'}$.

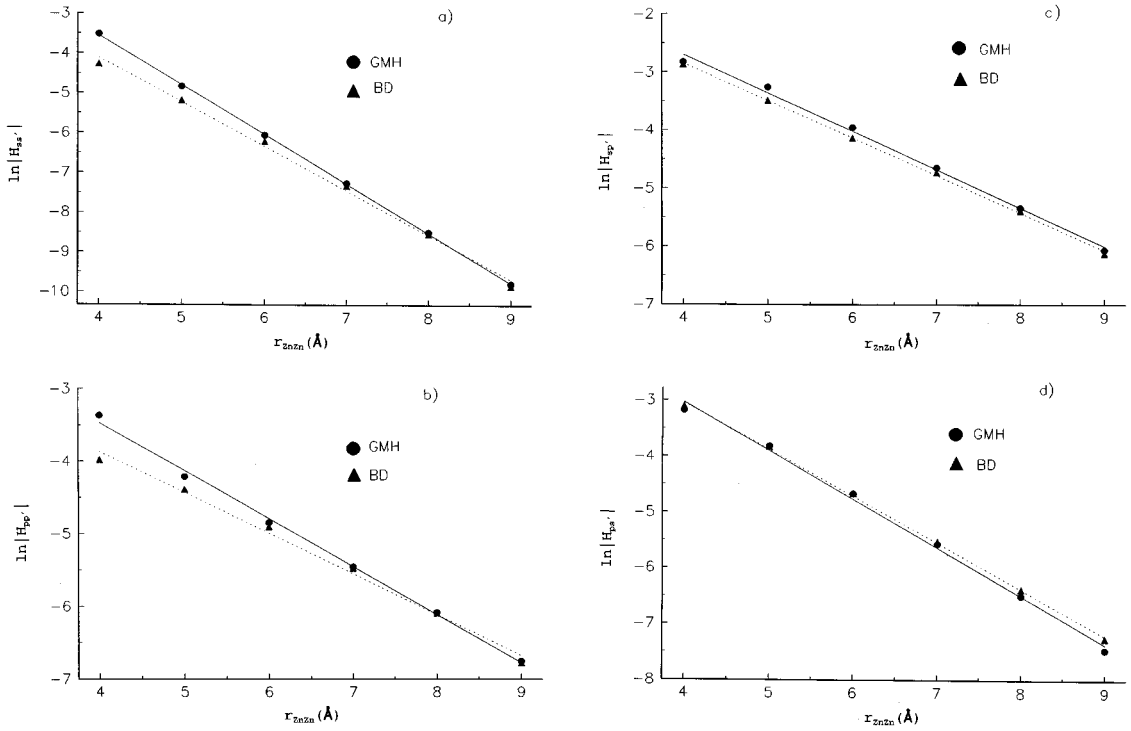

FIG. 3. Plot of $\ln|H_{ab}|$ vs r_{ZnZn} for $Zn_2(H_2O)^+$ based on the GMH (circles) and BD (triangles) methods, $r_{\mathrm{ZnO}}=3.05$ Å: (a) $H_{ss'}$, (b) $H_{pp'}$, (c) $H_{sp'}$, (d) $H_{ps'}$.

smaller than their counterparts for Zn_2^+ (Table II), as expected qualitatively from trends in IP's [Table I and Eq. (8)]. In a similar fashion we find $\beta_{sp'}<\beta_{ps'}$ as expected. We note that the agreement between GMH and BD results for $r_{\mathrm{ZnO}}=3.05$ Å (Table III B) is somewhat better than that found at $r_{\mathrm{ZnO}}=2.05$ Å (Table III A), and we discuss the reasons for this in Sec. V. The decay constants for $r_{\mathrm{ZnO}}=3.05$ Å are somewhat different from those for either the symmetrical Zn_2^+ (i.e., $r_{\mathrm{ZnO}}=\infty$) system or the systems with $r_{\mathrm{Zn-O}}=2.05$ Å, but this is expected given the different energy gaps obtained (see Table IV).

c. Assessment of the Condon approximation. The finding of similar H_{ab} magnitudes for different r_{ZnO} values, for a given type of process at a fixed value of r_{ZnZn}, lends support for the use of the Condon approximation in systems of this type. This possibility prompted a more detailed assessment using the GMH approach (Table V), with $r_{\mathrm{Zn-Zn}}$ held fixed at 5.0 Å while $r_{\mathrm{Zn-O}}$ was varied from 2.05 to 100 Å. It is seen that a given matrix element varies as much as 50% over this range, with some instances of significant nonmonotonic behavior, especially for the $s-p'$ and $p-p'$ matrix elements (see discussion in Sec. V). Nevertheless, the overall variations of H_{ab} for a given orbital type may still be considered relatively modest in view of the sizable variation of IP ($\sim$1 to 2 eV) with respect to r_{ZnO} (Table I).

d. Sensitivity to details of projector states. One might wonder how sensitive the matrix elements obtained from the BD procedure are to the choice of reference diabatic orbitals and/or CI coefficients in the definition of the diabatic projector states, $\psi_j^{P^0}$ (see Sec. II and Ref. 27). To test the sensitivity to the choice of diabatic orbitals we have performed additional calculations in which the reference orbitals were taken as the ANO's for the system with r_{ZnZn} greater than that for the actual system of interest by 1 Å, in contrast to the procedure used above, in which the reference ANO's were always obtained for $r_{\mathrm{ZnZn}}=20$ Å. We found at most a 3% difference in β between the two methods of defining the diabatic orbitals. To test the sensitivity to the choice of projector coefficients, we carried out further calculations using the full set of CI coefficients for each adiabatic state within the n_p space of diabatic CSFs at large r, rather than zeroing out the small contributors from the CSF's other than the dominant one. The largest change in β values resulting from this means of defining projectors was 7% ($s-s'$ transfer),

TABLE V. GMH electronic coupling elements for $Zn_2H_2O^+$ vs r_{ZnO}, with $r_{\mathrm{Zn-Zn}}=5.0$ Å.[a]

r_{ZnO} (Å)	$H_{ss'}$	$H_{pp'}$	$H_{sp'}$	$H_{ps'}$
2.05	10.5	13.0	51.7	22.3
2.25	10.1	15.0	55.5	22.0
2.55	9.07	15.5	50.0	21.9
2.85	8.28	15.1	42.5	22.0
3.05	7.95	14.7	38.5	22.1
4.05	7.27	13.6	29.2	22.6
6.05	6.95	13.1	25.2	23.1
100[b]	6.85	12.9	23.7	23.7

[a]All values in mhartree, based on 3/12 4SA/CASSCF wave functions, and are in atomic units.

[b]These values supersede the values listed for $r_{\mathrm{ZnO}}=\infty$ in Table I of Ref. 18(a).

TABLE VI. Two-state GMH and MH electronic coupling elements for $Zn_2OH_2^+$ vs r_{ZnZn}, with $r_{Zn-O}=3.05$ Å.[a]

r_{ZnZn} (Å)	Method	$H_{ss'}$	$H_{pp'}$	$H_{sp'}$	$H_{ps'}$
4.0	GMH	17.7	12.6	85.8	38.9
	MH	12.1	7.35	25.3	14.1
5.0	GMH	6.66	13.4	42.3	20.5
	MH	5.63	8.34	25.4	14.4
6.0	GMH	2.21	7.69	19.8	9.10
	MH	2.00	5.87	15.1	7.80
7.0	GMH	0.682	4.24	9.70	3.77
	MH	0.642	3.54	8.17	3.47
8.0	GMH	0.201	2.27	4.81	1.50
	MH	0.193	2.01	4.28	1.42
9.0	GMH	0.0555	1.16	2.32	0.572
	MH	0.0538	1.07	2.15	0.551
β[b]	GMH	2.31	1.19	1.46	1.70
	MH	2.19	0.82	1.05	1.37

[a]The results were obtained from 3/12 4SA/CASSCF calculations. The MH Refs. 18(c)–18(h) result is based on $r_{DA}^0=r_{ZnZn}$. See the text for other details.
[b]See Table II for details.

with the remaining β values affected to a much smaller degree. The absolute values of the matrix elements were also quite similar, irrespective of the particular choices considered here for defining the reference diabatic states. This suggests that in general, the results for coupling elements may not be strongly affected by choices regarding fine details of this type.

e. Comparison of two-state and four-state results. All of the results for $Zn_2(H_2O)^+$ discussed so far (Tables III–V) are based on a multistate treatment ($n_p=4$). It is now of interest to compare these results with those based on the familiar two-state approximation, i.e., where each of the four processes of interest [Eq. (7)] is treated in terms of the appropriate pair of adiabatic states (a subset of the full space of four states). In addition, within the two-state framework it is of interest to compare the GMH model [Eq. (2)][18(a)] with its predecessor, the MH model[18(e)–18(h)] [Eq. (1)], in which $\Delta\mu_{ab}$ is equated to er_{Zn-Zn} and ΔE_{ab} is replaced with the appropriate adiabatic energy gap (ΔE_{12}).[18(g)–18(h)] Table VI addresses these questions, with GMH and MH results based on $r_{ZnO}=3.05$ Å. In comparison with the results from Table III B it is seen that at large r_{Zn-Zn} either two-state approach yields results in excellent agreement with the multistate treatments. At short r_{Zn-Zn} significant differences are observed between these and the full four-state GMH, to which they are approximations. In particular, for both two-state approaches the increase of H_{ab} with decreasing r_{Zn-Zn} is slower than that given by the four-state GMH, and for the $s-p'$ element the MH result decreases more rapidly between 4 and 5 Å than either of the GMH results. It is interesting to note that at short r_{Zn-Zn} the two-state GMH actually agrees better with the BD results than it does with the four-state GMH. We return to the relative merits of the GMH and BD results in Sec. V.

TABLE VII. GMH and BD electronic coupling elements for the benzene–Cl system with $d=0.6$ Å and 1.208 Å ($r=3.00$ Å).[a]

		H_{ab}		
Method	d (Å)	H_{2pz}[b]	H_{2py}[b]	H_{2px}[b]
GMH	0.6	15.2	18.5	17.3
BD	0.6	16.1	17.0	14.9
GMH	1.208	24.1	14.7	13.1
BD	1.208	26.2	14.0	6.04
BD[c]	1.208	24.4	14.1	11.3

[a]Results from 9/5 5SA/CASSCF calculations in a split valence (VDZ) atomic natural orbital basis (Ref. 36). All values in mhartrees (see the text for details of geometry and matrix elements). Unless otherwise specified, the projection vectors for the BD analysis are the dominant diabatic configurations (χ_j^0).
[b]The H_{ab} values are denoted according to the dominant Cl orbital-type involved in each case.
[c]Projection vectors based on the CI representation of the diabatic state at large r (i.e., including contributions from all (n_p) of the dominant CSF's).

C. Benzene+Cl

As another example of the application of the GMH and BD methods, we consider briefly the case of *et* between benzene and Cl in a complex of the π-type, with C_s symmetry, as described in Sec. III B. Specifically, we place the Cl atom 3 Å above the benzene plane, either directly over a CC bond ($d=1.21$ Å) or halfway between this point and the six fold local axis of benzene ($d=0.6$ Å). Reference diabatic orbitals were obtained at $r=7$ Å and $r=5.5$ Å, respectively (little sensitivity to the particular large d value for the calculation of reference diabatic orbitals is expected in this range). As shown in Table VII, the GMH and BD methods give quite similar results for the various electronic coupling elements at a given d, and comparison of values for the two different d's shows the sensitivity of H_{ab} to Cl position over the benzene ring, especially for *et* involving the $2p_z$ orbital of Cl [the three lowest-lying states in order of increasing energy are dominated, respectively, by holes in the $2p_z$, $2p_y$, and $2p_x$, manifold of the Cl atom, given the coordinate system adopted here (see Sec. III B)]. In tests using other geometries we find that the GMH and BD methods yield similar agreement. Also included for $d=1.21$ Å are values of H_{ab} obtained from projectors ($\psi_j^{P_0}$, see Sec. II B) based on all n_p CSFs in the large r CASSCF wave function. It is seen that the H_{2pz} and H_{2py} elements are insensitive to this change, but the H_{2px} varies by approximately a factor of 2. This sensitivity arises largely from the near-degeneracy of the Cl p orbitals and the significant difference in magnitude of the p_x and p_z matrix elements. In additional calculations[39] we have shown that consideration of the first two states with local benzene triplet character has little effect on the matrix elements dealt with here.

V. DISCUSSION

The first point to be made about the above results is the similarity between the GMH and the BD coupling matrix elements, both with respect to magnitude and decay with distance. The GMH and BD methods offer independent

TABLE VIII. Effective charge transfer distances ($|\Delta\mu/e|$) for processes in $Zn_2H_2O^+$ ($r_{ZnO}=3.05$ Å).[a]

r_{ZnZn} (Å)	State definition	Process ss'	pp'	sp'	ps'
4.0	diabatic[b] GMH	4.05	2.88	3.29	3.63
	BD	4.13	2.72	3.25	3.59
	adiabatic[c]	0.95	0.44	0.47	0.93
	noninteracting components[d]	4.00	3.97	3.97	4.00
5.0	diabatic[b] GMH	4.67	3.60	3.88	4.40
	BD	4.68	3.56	3.85	4.39
	adiabatic[c]	3.49	2.27	2.57	3.20
	noninteracting components[d]	5.00	4.97	4.97	5.00
8.0	diabatic[b] GMH	7.68	7.08	7.15	7.60
	BD	7.68	7.08	7.15	7.60
	adiabatic[c]	7.67	7.02	7.11	7.58
	noninteracting components[d]	8.00	7.97	7.97	8.00

[a]All parameters are given in Å units.
[b]$\Delta\mu\equiv\Delta\mu_{ab}$, using state labels introduced in Sec. I.
[c]$\Delta\mu\equiv\mu_1-\mu_2$, where i,j are the labels of the adiabatic states which correspond to the diabatic pairs a,b.
[d]$\Delta\mu$ obtained by superposition of charge densities for noninteracting components (i.e., $Zn+Zn(H_2O)^+$ or $Zn^++Zn(H_2O)$, with the neutral species in the ground state or lowest triplet state, depending on the particular process).

means for defining and calculating H_{ab}, and the fact that they yield results in generally close agreement lends support to the concept of diabatic state properties. In addition, the comparisons with the values obtained for the symmetric system, Zn_2^+, where a third means of estimating the coupling can be used lends further support to the utility of the methods. The comparison of two-state GMH (or Mulliken–Hush) H_{ab} values for $Zn_2(H_2O)^+$ with those from the multi- (i.e., four) state GMH and BD values shows that a simple pairwise (i.e., two-state) approach may be adequate when the $D-A$ interactions are relatively weak. However, even in the weak coupling regime, the treatment of the ''cross reactions'' ($H_{sp'}$ and $H_{ps'}$) at the two-state level requires nonequivalent D and A sites (achieved here by the H_2O ligand at one of the Zn sites).

A. Effective *et* distances (r_{DA})

Aside from direct consideration of H_{ab} values, a convenient way to compare the GMH and BD results and to place them in perspective is to examine the dipole moment shifts ($\Delta\mu$) associated with the four types of *et* processes given in Eq. (7). Table VIII displays $\Delta\mu$ values for $Zn_2(H_2O)^+$ at three different r_{ZnZn} values (4, 5, and 8 Å) and with r_{ZnO} fixed at 3.05 Å. The $\Delta\mu$ values are actually presented as the scaled quantities ($|\Delta\mu/e|$) corresponding to effective charge transfer distances (r_{DA}), which may be compared with the ''zeroth-order'' *et* separations given by r_{ZnZn}. The diabatic quantities in Table VIII (both GMH and BD) may be compared on the one hand with the corresponding adiabatic quantities, $|\Delta\mu_{ij}/e|$ for the i,j pair of adiabatic states, and on the other hand with the reference r_{DA} values based on the dipole moments of the systems obtained by the superposition (at the appropriate r_{ZnZn} value) of the separate species ($Zn+ZnH_2O^+$ or Zn^++ZnH_2O). At all values of r_{ZnZn} the same qualitative pattern is evident for each of the four *et* types: relative to the result for the superposed noninteracting species, the diabatic r_{DA} values are somewhat reduced, while the $D-A$ mixing implicit in the adiabatic results yields further reduction, increasingly so as r_{ZnZn} is reduced from 8 to 4 Å. In all cases, the GMH and BD results are very similar. The diabatic r_{DA} values are in general less that r_{ZnZn}, differing by up to 30%.

TABLE IX. Results from six-state GMH and BD analyses ($r_{ZnZn}=8.0$ Å).[a]

r_{ZnO} (Å)	Matrix element	ss'	pp'	sp'	ps'
2.05	H_{ij}^{GMH}	0.0454	3.55	2.14	0.530
	H_{ij}^{BD}	0.299	1.65	4.81	2.66
	$\lvert\Delta\mu_{ij}^{GMH}/e\rvert$	7.63	8.76	8.76	7.64
	$\lvert\Delta\mu_{ij}^{BD}/e\rvert$	7.55	8.79	8.96	7.38
	$\lvert\Delta\mu_{ij}^{adiabatic}/e\rvert$	7.63	6.38	6.49	7.53
	$\lvert\Delta\mu_{ij}^{noninteracting}/e\rvert$	8.25	9.66	9.66	8.25
3.05	H_{ij}^{GMH}	0.233	3.31	1.91	0.494
	H_{ij}^{BD}	0.224	3.56	2.46	3.52
	$\lvert\Delta\mu_{ij}^{GMH}/e\rvert$	7.72	7.66	7.54	7.84
	$\lvert\Delta\mu_{ij}^{BD}/e\rvert$	7.91	7.57	7.91	7.80
	$\lvert\Delta\mu_{ij}^{adiabatic}/e\rvert$	7.67	7.02	7.11	7.58
	$\lvert\Delta\mu_{ij}^{noninteracting}/e\rvert$	8.00	7.97	7.97	8.00

[a]Hamiltonian matrix elements in mhartrees, $|\Delta\mu_{ij}/e|$ values in Å. All results obtained from GMH or BD analyses based on a 3/12 6SA/CASSCF calculations. See the text for details.

B. Comparison of GMH and BD results

In spite of the good overall correspondence, some appreciable differences are found between the GMH and BD H_{ab} values in the Zn_2^+ and $Zn_2(H_2O)^+$ systems. We analyze these differences in terms of various assumptions underlying the GMH and BD approaches, as formulated in Sec. II. The GMH method is intended for long range, where the distance scale for transfer (r_{DA}) is large relative to that for the local D and A sites. Since the effective radial extent of the Zn sites may be taken as ~ 2 Å, based on calculated rms radii for the $4s$ and $4p$ valence orbitals of Zn, we see (e.g., cf. Table VIII) that the assumed separation of distance scales is not strictly obeyed for the shorter range of r_{ZnZn} values (near 4 Å), and this fact helps to account for differences in GMH and BD results for $r_{ZnZn}=4$ Å (other factors operative also at larger ZnZn separations for the case of $Zn_2(H_2O)^+$ with $r_{ZnO}=2.05$ Å are discussed below). A useful diagnostic for this lack of separation of distance scales is found in the transformed BD dipole moment matrix. Inspection of the full dipole moment matrices in the diabatic representation obtained by the BD procedure (not shown) reveals that in most cases dipole matrix elements linking states associated with different sites have very small magnitude ($<10\%$ of the corresponding adiabatic values), thus justifying the neglect of such elements in the formulation of the GMH method [Sec. II A and Ref. 18(a)]. In some cases, one finds the two-center BD μ_{ij} matrix elements to be reduced relative to the corresponding adiabatic matrix element, but still sizeable relative to the adiabatic value. When this is the case, the MH or GMH treatments will tend to yield inaccurate results for the

electronic coupling when applied at the given distance (e.g., an overestimate for H_{ab} when the direct and MH contributions to μ^{ad} are of the same sign).

C. Choice of adiabatic state space

Another important assumption underlying the present formulation of diabatic states is the separation of diabatic state energies from those of states lying outside the adopted P space. Expansion of the number of adiabatic states used in the nSA/CASSCF (and also the GMH or BD analysis) beyond 4 (to 6) reveals that for $Zn_2(H_2O)^+$ with $r_{ZnO}=2.05$ Å there is a near-degeneracy (diabatic energy separation of ~ 0.005 h) between states dominated by ^3P character on ZnH_2O and ^1P character on the Zn atom, such that the fourth adiabatic state is a strong admixture of these two diabatic states. This result helps to explain the fact that for this r_{ZnO} both BD and GMH tended to yield diabatic $\Delta\mu_{ij}/e$, where i or j involves the local ^3P state on $Zn(H_2O)$, that were significantly smaller than r_{ZnZn}. In order to obtain more nearly localized states in the GMH sense, then, one might expand the adiabatic state space. In fact, in test calculations with an expanded state space (including states with ^1P-like character on both the Zn and ZnH_2O sites) we find significantly more localized Zn ^3P states, smaller values of $H_{sp'}$, and larger values for $\Delta\mu_{ij}/e$ (Table IX). Since our main goal here has been to compare the GMH and BD methods, we have not focused on such an expanded state space. When $r_{ZnO}=3.05$ Å, the four-state assumption is on firmer ground, since for the pair of diabatic states just discussed (i.e., those with dominant $^3P Zn(H_2O)$ and ^1P Zn character) the corresponding energy separation is nearly three times as large, and the diabatic states tend to be more localized for $n=4$.

D. The Condon approximation

The data in Table V shows that H_{ab} magnitudes do not vary strongly with the ZnH_2O separation in the $Zn_2(H_2O)^+$ complex, thus giving some qualitative support for the use of the Condon approximation. Nevertheless, at the quantitative level appreciable variation with r_{ZnO} is observed, especially for $H_{ss'}$ and $H_{sp'}$, where overall reductions by a factor of about 2 are observed over the full range of r_{ZnO}. For the coupling involving p or p', examples of nonmonotonic variation are found. To the extent that the Condon approximation is valid, one may often employ techniques such as external electrostatic fields or geometric variation so as to minimize the adiabatic splitting, ΔE_{12}, thereby permitting H_{ab} to be estimated as one-half this minimum value, as noted in Sec. I. However, we reiterate that one of the strengths of the GMH or BD approaches is the applicability to an arbitrary configuration of the system.

E. Complementary aspects of the GMH and BD approaches

To the extent that different diabatization schemes (in the present case, GMH and BD) yield coupling elements of differing magnitude, we emphasize that there is no *a priori* basis for deciding which scheme has greater validity. In the present context of *et* processes, an important criterion of utility for a given set of diabatic states is their ability to serve as initial and final states in a reliable quantitative formulation of thermal et rate constants for weakly coupled $D-A$ systems.[1] Coupling elements inferred from the GMH (or related MH) formulation of diabatic states have been successfully employed in rationalizing experimental kinetic data,[2,24] including a recent example of photoinduced data,[16] and the demonstration here that similar coupling elements may be obtained from an independent formulation (BD), underscores the robustness of diabatic formulations based on quantum chemical concepts.[43]

The two methods presented here for the evaluation of the electronic coupling elements (GMH and BD), in addition to providing a useful basis for assessing the sensitivity of diabatic state properties to alternative choices of such states, also serve complementary roles to some extent when it comes to ease of applicability. Computationally, the GMH method is significantly easier to implement, as long as one can evaluate the full dipole moment matrix for the calculated eigenstates (or obtain it from experimental data[1(b),18(a)]). The BD method can be used where dipole moments are not available, but requires some care in the definition of reference (noninteracting) states. These states may be obtained at a point of high symmetry[20] or one where the donor and acceptor are well separated (the procedure employed in the present study). This is relatively simple to do when the donor and acceptor are not covalently bound or when a geometric parameter (say, for example, a twist angle) can at some point naturally decouple the diabatic states. When these conditions do not pertain it is somewhat more difficult to define diabatic states using the BD method.[26] The GMH model avoids the need for explicit reference states, and this feature makes it an attractive method to use for rigidly linked donor and acceptor systems.[16]

Finally, while the GMH model is designed specifically to describe charge transfer reactions involving well-separated charge-localized states, the BD method has greater generality and may be applied to a variety of chemical processes,[19,20] including triplet energy transfer, a two-electron process closely related to electron (and hole) transfer.[43]

F. Advantages of the GMH and/or BD methods vis-a-vis alternative approaches

We have already noted (Sec. I) a variety of problems associated with other schemes for obtaining *ab initio* and/or all-valence-electron semiempirical estimates of electronic coupling elements, including the limitation of being restricted to the diabatic crossing point (either for symmetric systems or artificially perturbed nonsymmetric systems), the difficulty in obtaining reliable estimates of H_{ab} when extensive electron correlation is employed, and the inability to treat several states at once. It is clear that the present methods circumvent the first difficulty, but it should also be clear from the above applications that they do not suffer from the latter two defects. In fact, the calculated results are found to be robust when more complete treatments of electron corre-

lation are used.[44] In addition, neither method is limited to the use of CASSCF wave functions, although as currently implemented the BD scheme does require a common set of orbitals. For either method one could use multireference singles and doubles CI or, for example, multireference second-order perturbation theories that allow for relaxation of the reference space weights upon correlation (such methods include the B_k method of Nitzsche and Davidson,[45] the multireference perturbation theories of Koslowski and Davidson[46] or Hoffmann[47] and various multistate perturbation theories and coupled-cluster theories.[48] While there has been no need to include extensive treatment of electron correlation in the cases dealt with here, the need may arise in more complex systems of experimental interest, and the current methods are capable of treating these cases as well. We note in passing that one can use the BD method to approximately correct single-state perturbation theories for the need to allow correlation to alter the weights of the reference space coefficients, thus yielding an approximate multistate perturbation theory.[49]

VI. CONCLUSIONS

We have tested and compared two methods for the calculation of electronic coupling elements controlling electron transfer reactions, discussing in detail the results of applications to the $Zn_2(H_2O)^+$ and benzene–Cl complexes. It is seen that the methods yield quite similar results for the coupling elements, and agree quite well with those obtained in the limiting case of a system where one can use an independent means (half the energy splitting of symmetric and antisymmetric states) for evaluating the matrix element. Tests of the Condon approximation indicate that it holds reasonably well over a large range of structural variations, although appreciable variations of H_{ab} with structure (including nonmonotonic behavior) were obtained in some cases. Diabatic dipole moment matrices obtained from the BD approach demonstrate that the magnitudes of off-diagonal elements (μ_{ab}) linking different sites are in general sufficiently small in comparison with the corresponding adiabatic values ($\leqslant 10\%$) to support one of the central tenets of the GMH method.[18]

ACKNOWLEDGMENTS

R.J.C. acknowledges support of this research from an NSF grant (CHE-9222822) and a Camille and Henry Dreyfus Teacher-Scholar award. The work carried out at BNL was performed under contract DE-ACO2-76CH00016 with the U.S. Department of Energy and supported by its Division of Chemical Sciences. R.J.C. is a Camille and Henry Dreyfus Teacher Scholar, 1993–1998. Work carried out in part while on sabbatical leave at Brookhaven National Laboratory, 1994–95.

[1] (a) M. D. Newton, Chem. Rev. **91**, 767 (1991); (b) M. D. Newton and R. J. Cave, in *Molecular Electronics*, edited by J. Jortner and M. A. Ratner (Blackwell Science, in press).
[2] R. A. Marcus and N. Sutin, Biochim. Biophys. Acta **811**, 265 (1985).
[3] I. R. Gould, R. H. Young, L. J. Mueller, A. C. Albrecht, and S. Farid, J. Am. Chem. Soc. **116**, 3147, 8188 (1994).
[4] (a) J. Halpern and L. E. Orgel, Discuss. Faraday Soc. **29**, 32 (1960); (b) H. M. McConnell, J. Chem. Phys. **35**, 508 (1961).
[5] S. Larsson, J. Am. Chem. Soc. **103**, 4034 (1981).
[6] (a) B. Källebring and S. Larsson, Chem. Phys. Lett. **138**, 76 (1987); (b) S. F. Fischer and P. O. Scherer, Chem. Phys. **115**, 151 (1987); (c) P. O. Scherer and S. F. Fischer, **131**, 115 (1989); (d) M. Plato, K. Möbius, M. E. Michel-Beyerle, M. E. Bixon, and J. Jortner, J. Am. Chem. Soc. **110**, 7279 (1988); (e) A. Warshel, S. Creighton, and W. W. Parson, J. Phys. Chem. **92**, 2696 (1988).
[7] R. J. Cave, D. V. Baxter, W. A. Goddard III, and J. D. Baldeschwieler, J. Chem. Phys. **87**, 926 (1987).
[8] (a) M. D. Newton, J. Phys. Chem. **95**, 30 (1991), and references cited therein; (b) **92**, 3049 (1988); (c) M. D. Newton in *Cluster Models for Surface and Bulk Phenomena*, edited by G. Pacchioni *et al.* (Plenum, New York, 1992); (d) M. D. Newton, J. Phys. Chem. **95**, 30 (1991); (e) A. Broo and S. Larsson, Chem. Phys. **161**, 363 (1992).
[9] M. D. Newton, K. Ohta, and E. Zhong, J. Phys. Chem. **95**, 2317 (1991).
[10] (a) K. D. Jordan and M. N. Paddon-Row, J. Phys. Chem. **96**, 1188 (1992); (b) K. Kim, K. D. Jordan, and M. N. Paddon-Row, *ibid*. **98**, 11 053 (1994).
[11] (a) L. A. Curtiss, C. A. Naleway, and J. R. Miller, J. Phys. Chem. **97**, 4050 (1993); (b) **99**, 1182 (1995).
[12] (a) C. Liang and M. D. Newton, J. Phys. Chem. **96**, 2855 (1992); (b) **97**, 3199 (1993).
[13] (a) M. Braga and S. Larsson, Chem. Phys. Lett. **213**, 217 (1993); (b) M. Braga, A. Broo, and S. Larsson, Chem. Phys. **156**, 1 (1991).
[14] P. Siddarth and R. A. Marcus, J. Phys. Chem. **96**, 3213 (1992).
[15] (a) M. A. Ratner, J. Phys. Chem. **94**, 4877 (1990); (b) see, for example, J. J. Regan, S. M. Risser, D. N. Beratan, and J. N. Onuchic, *ibid*. **97**, 13 083 (1993), and references cited therein.
[16] R. J. Cave, M. D. Newton, K. Kumar, and M. B. Zimmt, J. Phys. Chem. **99**, 17 501 (1995).
[17] (a) I. Shavitt, in *Modern Theoretical Chemistry*, Vol. 3 Methods of Electronic Structure Theory, edited by H. F. Schaefer, III (Plenum, New York, 1977), p. 189; (b) D. K. W. Mok, R. Neumann, and N. C. Handy, J. Phys. Chem. **100**, 6225 (1996).
[18] (a) R. J. Cave and M. D. Newton, Chem. Phys. Lett. **249**, 15 (1996); (b) in footnote 5 of Ref. 18(a), ''$2\sqrt{\beta}$'' should be replaced with the correct expression, ''$\sqrt{2}\beta$''; the GMH model is an extension of the earlier two-state Mulliken–Hush model (Refs. 18(c)–18(f)); (c) R. S. Mulliken, J. Am. Chem. Soc. **64**, 811 (1952); (d) R. S. Mulliken and W. B. Person, *Molecular Complexes* (Wiley, New York, 1969); (e) N. S. Hush, Prog. Inorg. Chem. **8**, 391 (1967); (f) N. S. Hush, Electrochim. Acta **13**, 1005 (1968); (g) J. R. Reimers and N. S. Hush, J. Phys. Chem. **95**, 9773 (1991); (h) C. Creutz, M. D. Newton, and N. Sutin, J. Photochem. Photobiol. A **82**, 47 (1994).
[19] (a) T. Pacher, L. S. Cederbaum, and H. Köppel, J. Chem. Phys. **89**, 7367 (1988); (b) L. S. Cederbaum, J. Schirmer, and H.-D. Meyer, J. Phys. A **22**, 2427 (1989); (c) T. Pacher, H. Köppel, and L. S. Cederbaum, J. Chem. Phys. **95**, 6668 (1991); (d) T. Pacher, L. S. Cederbaum, and H. Köppel, Adv. Chem. Phys. **84**, 293 (1993); see also V. Sidis, *ibid*. **82**, 73 (1992).
[20] (a) W. Domcke and C. Woywood, Chem. Phys. Lett. **216**, 362 (1993); (b) W. Domcke, C. Woywood, and M. Stengle, *ibid*. **226**, 257 (1994).
[21] W. Jarzeba, K. Thakur, A. Hormann, and P. F. Barbara, J. Phys. Chem. **99**, 2016 (1995).
[22] Additional comparative studies are currently underway for systems which include through-bond (TB) coupling of $D-A$ sites via superexchange mechanisms (Ref. 1).
[23] (a) H.-J. Werner and W. Meyer, J. Chem. Phys. **74**, 5802 (1981); (b) A. Macias and A. Riera, J. Phys. B **11**, L489 (1978); (c) S. Kato and Y. Amatatsu, J. Chem. Phys. **92**, 7241 (1990); (d) H. J. Kim, R. Bianco, B. J. Gertner, and J. T. Hynes, J. Phys. Chem. **97**, 1723 (1993); (e) F. A. Gadea and M. Pelissier, J. Chem. Phys. **93**, 545 (1990).
[24] M. D. Newton and N. Sutin, Annu. Rev. Phys. Chem. **34**, 437 (1984).
[25] B. O. Roos, Adv. Chem. Phys. **69**, 399 (1987).
[26] An alternative method for the formulation of diabatic orbitals entails use of the GMH method. Given a set of adiabatic states spanning the localized (diabatic) states of importance for the processes in question, one first performs a GMH analysis to obtain the GMH diabatic states. Formation of the natural orbitals (based on the one-electron density) for each of the

GMH diabatic states yields, in the CASSCF active space, localized natural orbitals. The localized natural orbitals from one of the states may be used directly as reference diabatic orbitals in the BD procedure, or it may be that the active spaces from two or more GMH diabatic states need to be combined in order to span the set of localized orbitals required to describe the system.

[27] (a) In certain cases, where more than one CSF contributes significantly to $\psi_j^{P_0}$, a reference diabatic state may be multiconfigurational. In these cases we define $\psi_j^{P_0}$ (i.e., the ''projector'') as the linear combination of the dominant CSFs obtained at large r_{ZnZn}. Projection of these multiconfigurational zeroth-order states onto the adiabatic CI vectors at a given geometry is performed analogously to the single-CSF case; (b) For doublets involving three half-filled orbitals there are two linearly-independent spin eigenfunctions, and hence two CSFs which are included in the projector.

[28] P. O. Löwdin, Adv. Quantum Chem. **5**, 185 (1970).

[29] Since the adiabatic states are obtained as eigenvectors of a CI matrix, the P and Q spaces are automatically orthogonal, independent of any rotations done within the P space.

[30] C. F. Bender and H. F. Schaefer III, J. Chem. Phys. **55**, 4798 (1977).

[31] In cases where the active space canonical molecular orbitals obtained from the nSA/CASSCF procedure (at points of high symmetry or large $D-A$ separation) are adequately localized on the sites of interest, they could be substituted for the ANO's and serve equally well as reference diabatic orbitals.

[32] MOLCAS versions 2 and 3, K. Andersson, M. P. Fülscher, R. Lindh, P.-A. Malmqvist, J. Olsen, B. O. Roos, and A. J. Sadlej, University of Lund, Sweden, R. A. Blomberg and P. E. M. Siegbahn, University of Stockholm, Sweden, V. Kellö, J. Noga, and M. Urban, Commenus University, Slovakia and P.-O. Widmark, IBM, Sweden, 1991.

[33] A. J. H. Wachters, J. Chem. Phys. **52**, 1033 (1970).

[34] R. C. Raffenetti, J. Chem. Phys. **58**, 4452 (1973).

[35] GAMESS is a general purpose electronic structure program. The original version of the program was assembled by M. Dupuis, D. Spangler, and J. J. Wendoloski. The current version is described in M. W. Schmidt, K. K. Baldridge, J. A. Boatz, S. T. Elbert, M. S. Gordon, J. H. Jensen, S. Koseki, N. Matsunaga, K. A. Nguyen, S. J. Shu, T. L. Windus, M. Dupuis, J. A. Montgomery, J. Comput. Chem. **14**, 1347 (1993).

[36] W. S. Benedict, N. Gailer, and E. K. Plyler, J. Chem. Phys. **24**, 1139 (1956).

[37] (a) P.-O. Widmark, P.-Å. Malmqvist, and B. O. Roos, Theor. Chim. Acta. **77**, 291 (1990); (b) P.-O. Widmark, B. J. Persson, and B. O. Roos, *ibid*. **79**, 419 (1991).

[38] When a larger atomic natural orbital basis is used for $H_2O(3s2pld/2slp)$, the first excited state of $Zn(OH_2)$ shows significant charge transfer character (active space natural orbital occupations of greater than 0.5 for an O-like natural orbital). Since the primary purpose of the water in this study is simply to break the symmetry of the two Zn atoms, we have used a minimum basis set water, in order to minimize charge transfer effects within $ZnOH_2$.

[39] More extensive studies, including consideration of ''sigma'' as well as ''pi'' complexes (Refs. 18(a) and 21), and the influence of solvation on the coupling (H_{ab}) and other energetics, will be reported elsewhere, R. J. Cave, Y.-P. Liu, and M. D. Newton (to be published).

[40] C. E. Moore, Atomic Energy Levels, Vol II, Natl. Bur. Stand. (U.S.) Circ 467 (1949).

[41] In the localized ANO pairs in the reference state nSA/CASSCF calculations carried out for $r_{\mathrm{ZnZn}}=20$ Å (see Sec. II A), slight numerical departures from symmetry equivalence were obtained. The listed $H_{sp'/ps'}$ values are accordingly obtained as mean values of $H_{sp'}$ and $H_{ps'}$ (in each case the members of a given pair differed by $<10\%$).

[42] J. R. Reimers and N. S. Hush, Inorg. Chim. Acta **226**, 33 (1994).

[43] M. E. Sigman and G. L. Closs, J. Phys. Chem. **95**, 5012 (1991).

[44] (a) Other formulations similar in spirit to the BD method employed here (Refs. 19 and 20) have been reported by Ruedenberg and co-workers (Refs. 44(b)–44(d)). We thank Professor Ruedenberg for supplying us with a copy of Ref. 43(d) prior to publication, and also for a number of helpful discussions; (b) K. Ruedenberg and G. Atchity, J. Chem. Phys. **99**, 3799 (1993); (c) G. Atchity and K. Ruedenberg, *ibid*. **99**, 3790 (1993); (d) K. Ruedenberg and G. Atchity, preprint.

[45] L. E. Nitzsche and E. R. Davidson, J. Chem. Phys. **68**, 3103 (1978).

[46] P. M. Kozlowski and E. R. Davidson, J. Chem. Phys. **100**, 3672 (1994).

[47] M. R. Hoffmann, Chem. Phys. Lett. **210**, 193 (1993).

[48] (a) D. Mukherjee and S. Pal, Adv. Quantum Chem. **20**, 292 (1989); (b) K. Jankowski, J. Paldus, I. Grabowski, and K. Kowalski, J. Chem. Phys. **97**, 7600 (1992); (c) L. Meissner and R. J. Bartlett, *ibid*. **91**, 4800 (1989); (d) L. Meissner, S. Kucharski, and R. J. Bartlett, *ibid*. **93**, 1847 (1990).

[49] Use of the BD transformation of the adiabatic nSA/CASSCF Hamiltonian matrix yields diabatic states as in the present application. Once one has obtained the CASSCF diabatic Hamiltonian matrix, the diagonal Hamiltonian matrix elements can be augmented with correlation energies obtained at a geometry where the diabatic states are noninteracting (e.g., a point of high symmetry or large distance). Rediagonalization of the augmented Hamiltonian matrix yields new adiabatic states based on the above diagonal dressing of the diabatic states. This procedure has been used to study the interaction of the low-lying triplet states of pyrazine as a function of bending, R. J. Cave (to be published).